Computers and Electronics in Agriculture 167 (2019) 105043

Contents lists available at ScienceDirect

Computers and Electronics in Agriculture

journal homepage: www.elsevier.com/locate/compag

Investigation of bio-aerosol dispersion in a tunnel-ventilated poultry house

Longhuan Du[a,1], Li Yang[b,1], Chaowu Yang[b,*], Robert Dominy[c], Chenming Hu[b], Huarui Du[b], Qingyun Li[b], Chunlin Yu[b], Lingzhi Xie[a], Xiaosong Jiang[b,*]

[a] College of Architecture and Environment, Sichuan University, Chengdu, China
[b] Sichuan Animal Science Academy, Chengdu, China
[c] Faculty of Engineering and Environment, Department of Mechanical & Construction Engineering, Northumbria University, Newcastle, UK

ARTICLE INFO

Keywords:
Bio-aerosol
Poultry house
Ventilation
Dispersion

ABSTRACT

Bio-aerosol concentrations in poultry houses must be controlled to provide adequate air quality for both birds and workers. High concentrations of airborne bio-aerosols would affect the environmental sustainability of the production and create environmental hazards to the surroundings via the ventilation systems. Previous studies demonstrate that several factors including the age of the birds, the housing configuration, the humidity and temperature would strongly affect the indoor concentration of bio-aerosols. However, limited studies are performed in the literature to investigate the bio-aerosol dispersion pattern inside poultry buildings. In order to fill a gap of the understanding of the bio-aerosol dispersion behavior, experimental measurements of the indoor bio-aerosol distribution are performed in a tunnel-ventilated poultry house in this paper. Meanwhile a three-dimensional computational fluid dynamics (CFD) model is built and validated to further investigate the effect of flow pattern, turbulence and vortex on the dispersion and deposition of the bio-aerosols. Furthermore, bio-aerosols with various diameters are also examined in the CFD model. It is found that higher concentrations of bio-aerosols are detected at the rear part of the house and strong turbulent flow resulting from the ventilation inlets enhances the diffusion and dispersion of bio-aerosols. Local vortex or disturbed flow is responsible for higher local concentration due to the re-suspension of settled bio-aerosols, which suggests that careful attentions should be paid to these locations during cleaning and disinfection. Results from present study contribute to the optimization of design and operation of the poultry houses from the standing point of reducing airborne bio-aerosol concentrations.

1. Introduction

Poultry is regarded as one of the most important sources of protein for humans. However, serious airborne pollutants during the breeding periods could affect the environmental sustainability of the operation and production efficiency (Banhazi et al., 2008). The gases, dust and micro-organisms, which is also addressed as bio-aerosols, would reduce the air quality within the poultry building and research in the literature had demonstrated that these air pollutants were associated with health risks for both birds and exposed workers (Cambra-Lopez et al., 2010). In addition, the emissions from the poultry buildings may negatively affect the general health of people living in close proximity to the poultry farms (Mostafa, 2011). The high concentrations of bio-aerosols, especially bacteria would affect parts of the respiratory system of the people and induce a number of symptoms and diseases including allergic and non-allergic rhinitis, bronchitis, asthma and asthma-like syndrome, etc. (Kirychuk et al., 2003). The degree of hazardousness of the airborne bio-aerosol in the poultry building depends not only on the pathogenicity of micro-organisms but also on the particle size which determines their ability to penetrate the respiratory tract according to previous studies (Brodka et al., 2012). Therefore the bio-aerosols arising from the poultry production should be carefully considered and treated both in the poultry farm design and operation stage.

Several authors demonstrated that the level of airborne bio-aerosols depended on the age of hens or broilers and stocking density of the birds (Oppliger et al., 2008; Vučemilo et al., 2007). Studies also showed the poultry production system including housing system with litter and house with cages were important (Kirychuk et al., 2003; Nimmermark et al., 2009; Saleh et al., 2003). Furthermore, the environmental variables such as air temperature and humidity were found to have significantly effects on the concentration of the airborne bio-aerosol and the air quality (Al Homidan et al., 1997). Moreover, ventilation rate

* Corresponding authors at: Sichuan Animal Science Academy, No.7, Niusha Road, Jinjiang District, Chengdu, Sichuan Province 610066, China.
E-mail addresses: cwyang@foxmail.com (C. Yang), xsjiang2017@163.com (X. Jiang).
[1] These authors contributed equally to this work.

https://doi.org/10.1016/j.compag.2019.105043
Received 18 January 2019; Received in revised form 25 September 2019; Accepted 4 October 2019

was believed to be an important factor which determines to a great extent the aerosol formation, concentrations and emissions (Banhazi et al., 2008). Some researchers held the view that higher ventilation rate could result in lower indoor bio-aerosol concentration (Brodka et al., 2012; Lai and Chen, 2006) while other researchers claimed that higher ventilation rate (higher velocity and turbulence level) would actually increase the indoor bio-aerosol concentration due to the re-suspension of settled particles (Qi et al., 1992; Banhazi et al., 2008). The conflicting conclusions in the literature demonstrate that the dispersion and fate of airborne bio-aerosols in indoor environments like the poultry house is still poorly understood and constitutes an area of much controversy and challenging research.

Due to the drawbacks of the experimental measurements such as high cost, time-consuming, limited measurement points and the prerequisite of the existence of an experimental building, few experimental studies were performed in the literature to provide a detailed investigation of the dispersion of the airborne bio-aerosols in poultry houses. Thanks to the fast development of computer technology, the computational fluid dynamics (CFD) technique was applied extensively in studying the environmental parameters of livestock buildings in the recent decade (Rong et al., 2016). However, it is noted that limited studies were conducted by using CFD to investigate the indoor bio-aerosol distribution in poultry houses. Therefore, in order to fill a gap of the understanding of the bio-aerosol dispersion, diffusion and deposition in poultry houses, a three-dimensional CFD model was built in present study according to the real dimensions of a tunnel-ventilated laying hen house. Studies were performed to examine the bio-aerosol dispersion and deposition from the perspective of indoor flow pattern, turbulence and vortex generation (eddies). The overall aims of this study are to:

- Attempt to build and validate a three-dimensional CFD model.
- Investigate the dispersion and deposition of airborne bio-aerosols in the poultry house by using the validated CFD model and compare the predicted results with those measured experimentally.
- Understand the roles that flow pattern, turbulence and vortex play in the dispersion and deposition of airborne bio-aerosols, which could guide the cleaning and disinfection of the poultry houses.

2. Material and methods

2.1. Experiments

2.1.1. The poultry house

The experimental measurements were performed in an experimental-oriented laying hen house, equipped with tunnel ventilation system as shown in Fig. 1. The dimensions of the building were length, 40 m, width, 9.2 m, height (suspended ceiling height), 2.5 m. This laying hen house was provided with 2 side-wall air inlets (or referred as tunnel inlets) located at the front end of the house. 3 fans were installed at the end wall of the house and there were in total 32 side-wall windows as shown in Fig. 1. For the 2 air inlets and all side-wall windows, a bottom hinged flap mechanism was used to control the opening angle, enabling a control range from 0° (fully closed) to 90° (fully open). More details about the dimensions of the laying hen house could be found in previous studies (Du et al., 2019).

In the house, there were 4 rows of animal occupied zone, each row had 3 tiers of cages raising approximate 3500 laying hens. Each row was 1.36 m apart and the total height of the 3-tier cage was 1.65 m. The bottom of the cage was set 0.5 m high from the ground as shown in Fig. 1b. In order to prevent the cold air, which cooled by the evaporative cooling system, blew directly towards the hens caged in the vicinity of the inlets, the air was designed to enter the house at a pre-set 35° as shown in Fig. 1b. However, due to a mechanical failure, 2 flaps at the inlet of the side-wall B could only be set at 50° Therefore, special attention was paid when creating the CFD model in order to exactly match the experimental conditions.

2.1.2. Instrumentation

In order to validate the CFD model, the air velocity distribution in the laboratory scale laying hen house was measured by using the calibrated portable multi-function air velocity meter (Model 9545, TSI, USA). The resolution of the TSI velocity meter is 0.01 m s^{-1} and the accuracy is ± 3% of the reading or ± 0.015 m s^{-1}. With regard to the measurement of the concentration of bio-aerosols, a six-stage Andersen sampler (Anderson Instruments, USA) was applied together with an air pump (SKC QUICKTAKE30, USA). The air was sampled through a plastic tube at the flow rate of 28.3 L/min and impacted onto 90 mm diameter plastic agar plates filled with nutrient agar. The plates were incubated for 24 h at 37° and the resulting colony forming units (CFUs) were counted.

2.1.3. Measurements

For validating the CFD model, the indoor air velocity distribution was measured by using the TSI meter at 15 different locations at 2 heights: (1) at the height occupied by the birds of the first tier (0.8m); (2) at the height occupied by the birds of the third tier (1.8 m). The schematic drawing of the measurement positions is shown Fig. 2. All the measurements were conducted at the middle of each aisle. The portable TSI meter was fixed on a mobile mast while the mobile mast was situated and moved from point 1 to 15 (see Fig. 2) remaining for about 250 s at each location. The measurements were then repeated for point 16–30. For the validation tests, the measurements were performed under two ventilation conditions: only the middle fan in operation and all three fans in operation. Moreover, the velocity at the air inlets and the outlet fans were also measured and recorded.

For all the measurements taken with the TSI meter, the sampling frequency was 0.2 Hz, and 50 samples were taken at each designed position. In order to reduce measurement noise, the 50 samples were therefore averaged providing standard deviation and the mean value was considered as the reading of the noted time interval.

With regard to the investigation of bio-aerosol dispersion and diffusion, only the middle fan was set in operation and the samplings were conducted at 10 locations at two heights (0.8 m and 1.8 m) as shown in Fig. 3. The samplings were performed at the middle of each aisle and the sampling time was 60 seconds for each point. Details of the coordinate information are shown in Table 1 and the origin of coordinate is shown in Fig. 1. Duplicate samples were collected at each location, which led to in totally 40 samplings recorded for one experimental campaign. The experiments were repeated three times within a week. It should be noted that before conducting each experiment the ventilation system was turned on for at least half an hour in order to ensure a steady indoor environment and flow. Moreover, the bio-aerosol concentration at the air inlets were examined for each experiment and all the results demonstrated negligible airborne bio-aerosols comparing with those measured inside the poultry house.

2.2. Numerical simulation

2.2.1. Model set-up

A three-dimensional CFD model was built based on the dimensions of the laying hen house as illustrated in Fig. 1. The triangular rooftop was not included in the numerical model since it has no effect on the indoor flow. The exhaust fans were considered as circles of diameter of 1.27 m. The inlets were accurately modeled by means of the coordinates of their corners and the flaps at the 2 inlets were also modeled according to the pre-set degrees (Fig. 1). For experimental measurements performed in present study, the side-wall windows were fully closed for both validation tests and the investigation of bio-aerosol dispersion, so these side-wall windows were not modeled.

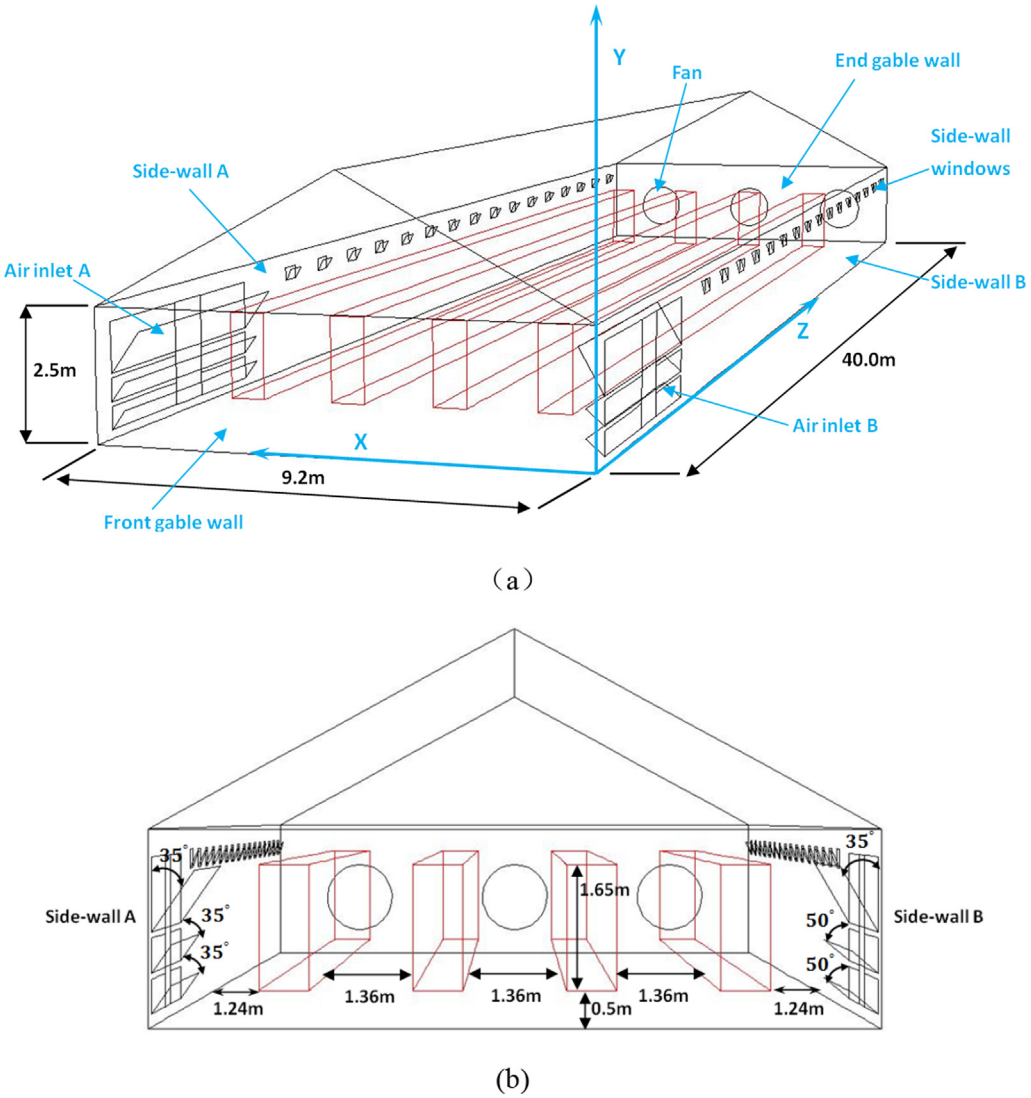

Fig. 1. Schematic drawing of the laboratory scale laying hen house (a) side view with the origin of coordinate used in present study, (b) front view. The animal occupied zone was simplified by red rectangular cuboids.

2.2.2. Porous media zone

In present study, it is unrealistic to model all birds discreetly in the geometry modeling and appropriate approximations were necessary to be made when building the CFD model. Therefore, in response to this issue, the porous media model had been applied to simulate the caged laying hen occupied zone, neglecting the feeding system, water supply system and manure removal system. 4 rectangular cuboids (Fig. 1) were created according to the actual dimension to represent the 3-tier caged laying hen occupied zones, which was later defined as porous media zones in Fluent 17.0. The idea of porous media is to add a source term in Navier-Stokes equations, which consist of two parts namely the viscous loss term and the inertial loss term.

By simplifying the caged laying hen occupied zone into porous media zone, it is crucial to find the correct viscous (D) and inertial (C) resistance coefficients. According to the recent study performed by Cheng et al. (2018) who investigated the resistance coefficient by CFD

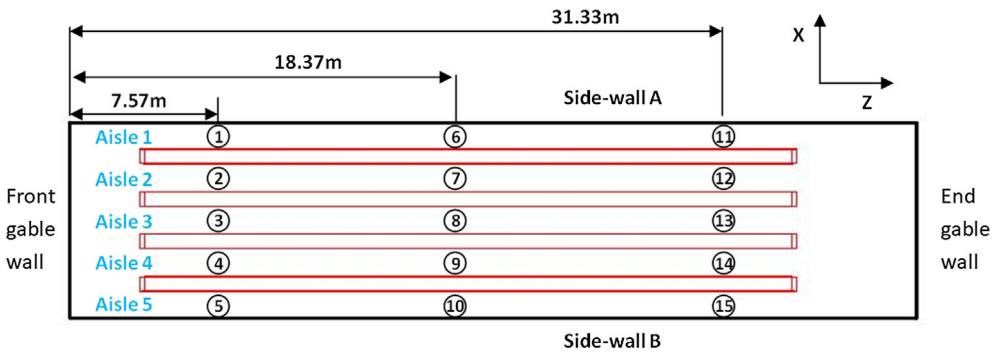

Fig. 2. Schematic drawing of measurement locations in the laying hen house at two heights: 0.8 m (No. 1–15) and 1.8 m (No. 16–30).

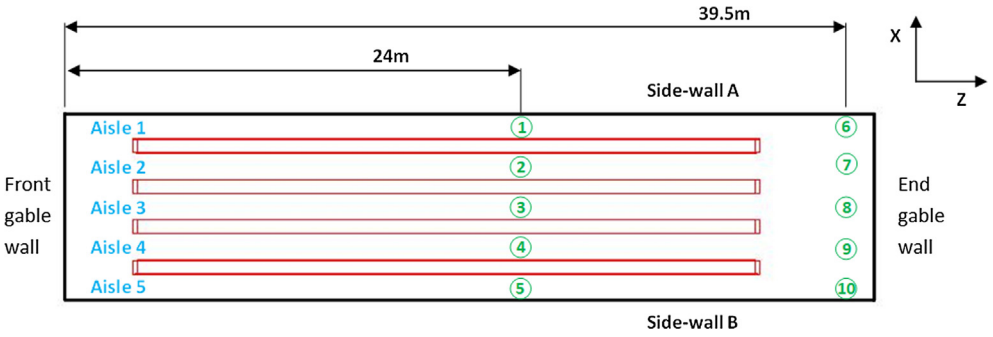

Fig. 3. Schematic drawing of bio-aerosol sampling positions at two heights: Y = 0.8 m (No. 1–10) and Y = 1.8 m (No. 1*–10*).

Table 1
The coordinate of the bio-aerosol sampling positions.

Sensor Number	X-coordinate (m)	Y-coordinate (m)	Z-coordinate (m)
1	8.58	0.8	24
1*	8.58	1.8	24
2	6.62	0.8	24
2*	6.62	1.8	24
3	4.6	0.8	24
3*	4.6	1.8	24
4	2.58	0.8	24
4*	2.58	1.8	24
5	0.62	0.8	24
5*	0.62	1.8	24
6	8.58	0.8	39.5
6*	8.58	1.8	39.5
7	6.62	0.8	39.5
7*	6.62	1.8	39.5
8	4.6	0.8	39.5
8*	4.6	1.8	39.5
9	2.58	0.8	39.5
9*	2.58	1.8	39.5
10	0.62	0.8	39.5
10*	0.62	1.8	39.5

Table 2
Resistance coefficient for porous media zone.

X-direction		Y-direction		Z-direction	
D_x, m^{-2}	C_x, m^{-1}	D_y, m^{-2}	C_y, m^{-1}	D_z, m^{-2}	C_z, m^{-1}
11381.2	0.82	22005.5	3.23	7121.5	2.27

simulation and wind tunnel measurements, it was found that the resistance coefficient was a function of bird geometry, distribution and weight. It should be noted that the density of occupants in Cheng et al.'s study (Cheng et al., 2018) was similar to the present study although the bird spatial distribution in the cage might change during the 2-hour experiment. Therefore, Cheng et al.'s study provides a reliable data source for present study to set up the porous media zone and the parameters used are shown in Table 2.

2.2.3. Grid convergence study

Due to the limitation of the computer power and time, it is impossible to obtain a CFD simulation result that independent of the computational grid especially for such a complicated 3-dimensional flow in a laying hen house. Therefore, it is meaningful to perform a grid convergence study to ensure the model could represent the actual house and provide reasonable results. The widely used uniform Grid Convergence Index (GCI) was adopted in this study to quantify the uncertainty of grid convergence. Details about the GCI could be found in reference (Roache, 1994).

4 different meshes, Mesh A (0.9 millions of cells), Mesh B (1.7 millions of cells), Mesh C (3.2 millions of cells) and Mesh D (5.5 millions of cells) were examined in this study by using the air velocity at four positions (P1, P2, P3 and P4) in the test zone. As shown in Table 3, by increasing the mesh cell numbers from 3.2 million (mesh C) to about 5.5 million (mesh D), limited GCI differences is found at P2, P3 and P4. Meanwhile the difference at P1 is also small with a GCI index of 6.47%. Therefore, taking the computing time and accuracy into consideration the Mesh C was chosen to perform the following studies.

Table 3
GCI calculated for velocity values of grid ratio r.

Points	Location			GCI		
	X	Y	Z	r = 1.56	r = 1.23	r = 1.19
P1	4.6	1.2	10	31.10%	22.02%	6.47%
P2	4.6	0.5	20	6.02%	3.56%	1.15%
P3	4.6	2	30	12.49%	6.32%	1.61%
P4	4.6	1.8	38	15.73%	8.69%	3.27%

Note: r = 1.19 is the mesh ratio from Mesh D to Mesh C, r = 1.23 is the mesh ratio from Mesh C to Mesh B, r = 1.56 is the mesh ratio from Mesh B to Mesh A.

2.2.4. Discrete phase model (DPM)

In order to investigate the dispersion and deposition of bio-aerosols, a Lagrangian particle tracking with stochastic discrete random walk (DRW) model was adopted to represent the eddy interactions of the discrete phase. The trajectory of the bio-aerosols was simulated by considering the change in particle velocity due to the particle inertia, gravity, drag force and Brownian motion. Previous studies (Zhao et al., 2004) demonstrated that for indoor aerosols, the lift force was comparatively small and therefore it was not considered in the present study. Several bio-aerosol diameters were examined in this study ranging from 1 μm to 100 μm and the particle velocities were assumed to be equal to the local mean fluid velocities at the particle release locations. A particle was deemed as deposited once it touched a solid wall surface and no re-suspension occurred ('trapped' boundary condition). Due to the uncertainties induced by DRW and Brownian force, the particle deposition for each particle size group was repeated 3 times for each test.

Since the animal occupied zones including caged birds, feeding system, water supply system and manure removal system could together be regarded as important bio-aerosol sources, therefore the bio-aerosols were released from 1000 point sources inside each row of the animal occupied zone at the height of Y = 1.33 m as schematically drawn in Fig. 4 (it should be noted that Y = 1.33 m was the middle height of the occupied zone). As the main aim of present study was to investigate the dispersion of the bio-aerosols, no special effort was made to exactly match the bio-aerosol generation rate and release locations with those in the real poultry house. Therefore, a constant release rate of 1×10^{-20} kg/s is adopted in this study. Moreover, this small release rate (mass input) is believed to have no effect on the flow.

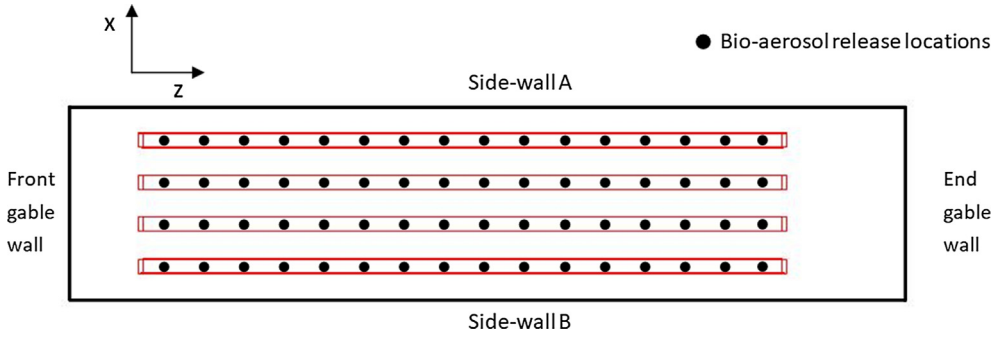

Fig. 4. Schematic drawing of the bio-aerosol release locations inside each row of animal occupied zone. The release rate is 1×10^{-20} kg/s.

2.2.5. Boundary settings and turbulence model

A non-slip condition was imposed for solid walls including the suspending ceiling, the floor, 2 side walls, the end and front walls so the fluid velocity at those surfaces was zero. A 'trap' boundary condition was also applied for above walls. In order to match the experimental condition, the boundary settings for the air inlets and outlet fans were chosen as pressure inlet and pressure outlet, respectively. The realizable k-ε turbulence model was applied due to its improvement on the prediction for flow rotation, recirculation and boundary separation (Rong et al., 2016) which were expected in this study. Standard wall function was employed, requiring the y^* value to be within 30 and 300 in the first cell. It was assumed that the CFD simulation was an incompressible, turbulent, 3-dimensional steady flow. Air properties were considered to be constant and the discretization scheme for pressure, momentum, energy, turbulent kinetic energy and dissipation rate was chosen as second order upwind.

3. Results and discussion

3.1. Model validation

In order to validate the CFD model built in this study, the simulation results of velocity distribution were compared with the filed measurements at the designed 30 points as shown in Fig. 2. Velocity at air inlets and outlets are measured and illustrated in Table 4. The validations were conducted under the middle outlet fan in operation and all three outlet fans in operation. It should be noted that during the field measurements the fluctuation of outside atmosphere condition was very limited based on the recordings.

The validation results are illustrated in Figs. 5 and 6. In order to avoid the large relative error which could arise when air velocities are relative small, previous studies (Blanes-Vidal et al., 2008) usually expressed the differences between measured and simulated air velocity in terms of $E_b = (|V_{CFD} - V_{EXP}|/V_0) * 100$, that is, as a percentage of the mean air velocity at the inlets (V_0) and this E_b is also adopted in present study. As demonstrated in Figs. 5 and 6, relative large discrepancies are found at the front part of the house at sensor numbers of No. 2–5 (and No. 17–20). These large discrepancies are probably related to the large turbulence and flow disturbance resulting from 2 strands of airflow (from side-wall inlet A and inlet B) collide at the middle of the house. For most points the difference is less than 10% and the corresponding mean E_b for the one-fan condition and three-fan condition is 5.67% and 5.85% respectively. It should be noted that this simplified CFD model does not include the feeding system, water supply system and manure removal system, which would to some extent responsible for the above discrepancies. Take the complexity of the flow into consideration, the above validation results are proved to be reasonable and satisfactory.

3.2. Indoor bio-aerosol distribution – Experimental measurements

The indoor concentration of airborne bio-aerosol was measured at 10 locations at two heights (0.8 m and 1.8 m) as shown in Fig. 3 and Table 1. During the sampling, only the middle outlet fan was in operation. Duplicate samples were collected at each sampling position and the averaged value is presented. The results of the number of colony forming units (CFUs) for the three tests are illustrated in Fig. 7, Fig. 8 and Fig. 9 respectively. Moreover, the assessment of *p*-values for significance differences in bio-aerosol concentrations depending on the sampling locations is shown in Table 5. According to these figures and the table, some interesting trend of the indoor bio-aerosol concentrations could be observed as follow:

- First of all, the three field tests all demonstrate that the concentration of bio-aerosols is higher at the end of the house (Z = 39.5 m). Table 5 clearly indicates that the mean value (M) at Z = 39.5 m is higher at both heights for each aisles ($p < 0.05$) comparing with the values measured at Z = 24 m. It is highly possible that for a tunnel-ventilated poultry house like the one shown in present study, the aerosols from skin, feather, feces, urine and feed would travel from upstream to the downstream inside the house. Some of the bio-aerosols would deposit on surfaces while others would finally be emitted from the outlet fans, which to some extent depends on the diameter of the bio-aerosol and the ventilation rate.
- Secondly, for Z = 24 m the bio-aerosol concentration seems to be higher at the middle aisles (Aisle 2, Aisle 3 and Aisle 4) comparing with that at aisles next to the side walls (Aisle 1 and Aisle 5) as

Table 4
Velocity at air inlets and outlets, ($m \cdot s^{-1}$).

Parameter	Location	Device	No. Samples	Mean(Standard deviation)
Air Velocity (Middle fan in operation)	Inlet-A	TSI Velocity Meter	50[a]	0.77 (0.04), 0.75 (0.04), 0.74 (0.04), 0.76 (0.03), 0.76 (0.04)
	Inlet-B	TSI Velocity Meter	50[a]	0.78 (0.04), 0.76 (0.04), 0.74 (0.04), 0.74 (0.04), 0.76 (0.04)
	Outlet Fan	TSI Velocity Meter	50[b]	6.23 (0.18), 6.19 (0.16), 6.20 (0.15)
Air Velocity (Three fans in operation)	Inlet-A	TSI Velocity Meter	50[a]	2.29 (0.02), 2.30 (0.03), 2.31 (0.02), 2.31 (0.05), 2.29 (0.03)
	Inlet-B	TSI Velocity Meter	50[a]	2.27 (0.03), 2.27 (0.03), 2.28 (0.02), 2.27 (0.03), 2.29 (0.02)
	Outlet Fan	TSI Velocity Meter	50[b]	6.22 (0.15), 6.31 (0.2), 6.24 (0.14)

[a] Velocity for each air inlet was measured at five points.
[b] Air velocity was measured at three points for the middle fan.

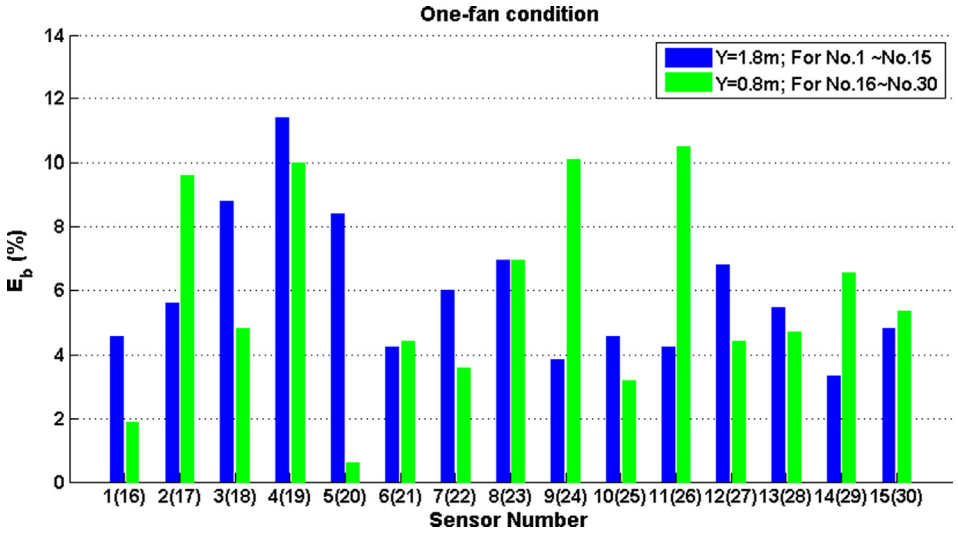

Fig. 5. The difference between simulated results and the experimental measurements at the designed 30 points expressed as E_b (%). One-fan condition.

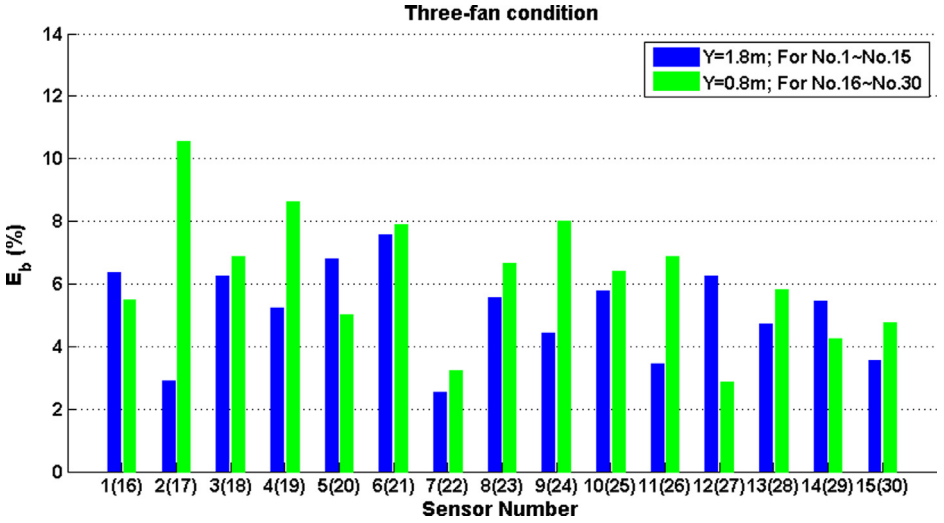

Fig. 6. The difference between simulated results and the experimental measurements at the designed 30 points expressed as E_b (%). Three-fan condition.

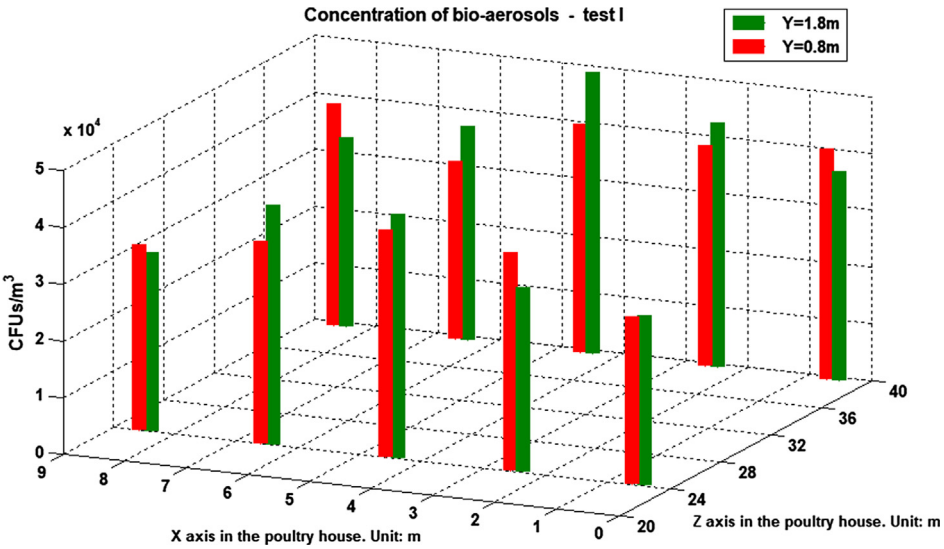

Fig. 7. Experimental measurement of indoor bio-aerosol concentration at designed locations at two heights (Y = 1.8 m and Y = 0.8 m) – test I.

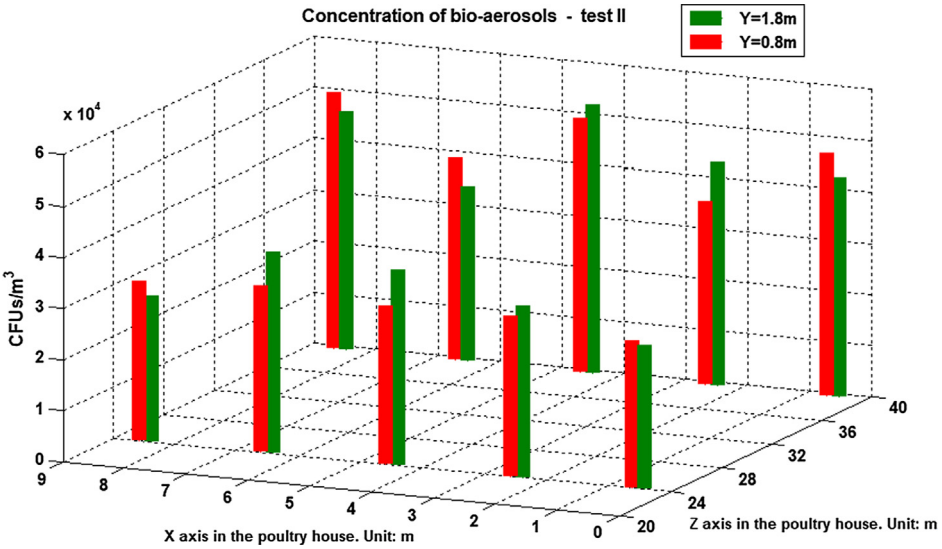

Fig. 8. Experimental measurement of indoor bio-aerosol concentration at designed locations at two heights (Y = 1.8 m andY = 0.8 m) – test II.

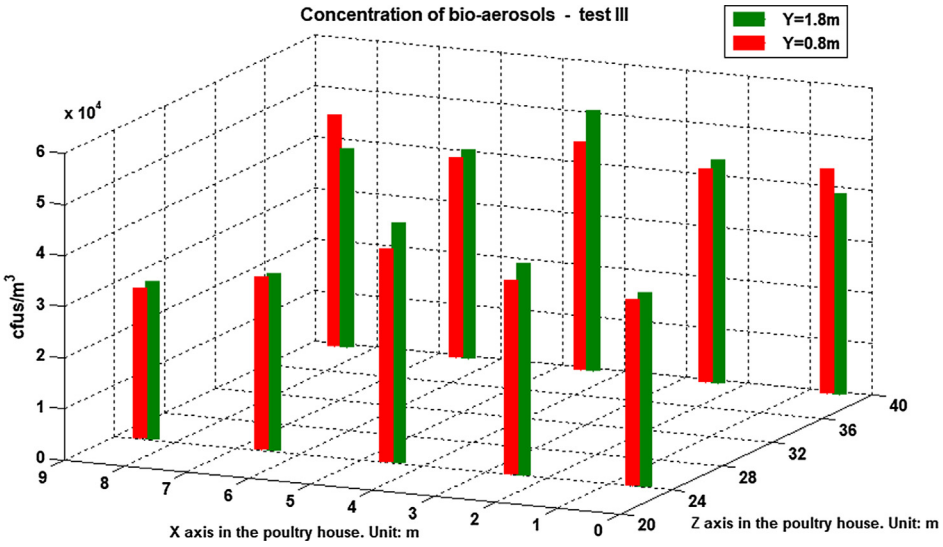

Fig. 9. Experimental measurement of indoor bio-aerosol concentration at designed locations at two heights (Y = 1.8 m andY = 0.8 m) – test III.

Table 5
Assessment of significance differences (*p*-value) in concentrations of bio-aerosols depending on locations.

Height	Z axis in the house	Aisle 1 M ± SD	Aisle 2 M ± SD	Aisle 3 M ± SD	Aisle 4 M ± SD	Aisle 5 M ± SD
Y = 1.8 m	Z = 39.5 m	$4.23 \pm 1.21^{b*}$	$4.28 \pm 1.14^{b*}$	$5.84 \pm 1.41^{a*}$	$4.70 \pm 0.99^{b*}$	$4.49 \pm 1.16^{b*}$
	Z = 24 m	3.04 ± 0.19^{b}	3.89 ± 0.55^{ab}	4.29 ± 0.55^{a}	3.59 ± 0.54^{ab}	2.98 ± 0.27^{b}
Y = 0.8 m	Z = 39.5 m	$4.93 \pm 1.06^{b*}$	$4.14 \pm 1.09^{b*}$	$5.19 \pm 1.49^{a*}$	$4.39 \pm 1.14^{b*}$	$4.83 \pm 1.13^{b*}$
	Z = 24 m	3.12 ± 0.31	3.41 ± 0.45	3.76 ± 0.55	3.59 ± 0.48	3.17 ± 0.40

Note:
1. The unit of bio-aerosol concentration is $\times 10^4$ CFU/m^3.
2. M±SD indicates the mean value (M) and the standard deviation (SD).
3. The data with same or no superscript letter (a, b) indicates no significance ($p > 0.05$) in a row.
4. The data with same or no superscript star (∗) indicates no significance ($p > 0.05$) in a column for Y = 1.8 m and Y = 0.8 m respectively.

illustrated in Figs. 7–9. Meanwhile as can be seen in Table 5, for Y = 1.8 m and Z = 24 m the middle aisles (Aisle 2, Aisle 3 and Aisle 4) indicate a significant difference ($p < 0.05$) comparing with aisle 1 and aisle 5, although it is not observed statistically for Y = 0.8 m. A possible explanation is that when the animal occupied zones are regarded as the sources of bio-aerosols, the aisles next to the side walls (Aisle 1 and Aisle 5) would face only one side of bio-aerosol sources while for those middle aisles the bio-aerosols would come from both sides, which is schematically indicated in Fig. 10.

- Thirdly, it is noted that for Z = 39.5 m the bio-aerosol concentrations at the corners of the house (Aisle 1 and Aisle 5) are relatively high, which are different from the situation at Z = 24 m as

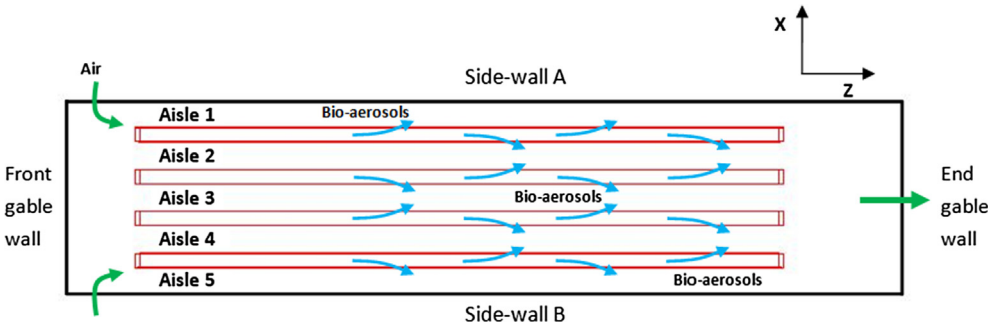

Fig. 10. Dispersion of bio-aerosols from animal occupied zones.

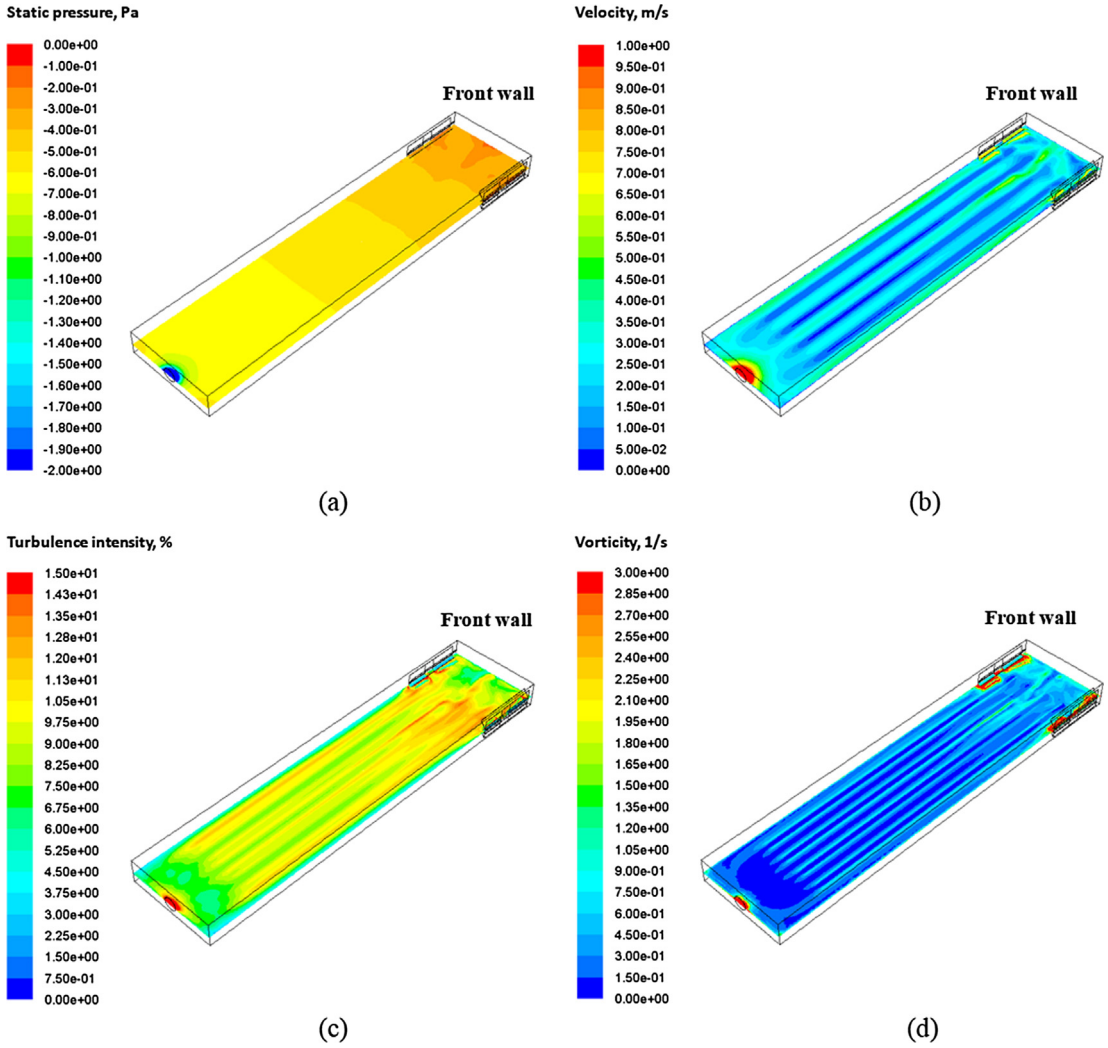

Fig. 11. CFD simulated indoor (a) static pressure, Pa, (b) velocity, m/s, (c) turbulence intensity, %, and (d) vorticity, 1/s. Y = 1.8 m.

discussed in above paragraph. Certain flow pattern might be responsible for these distributions but it is hard to be studied by using traditional experimental tools.

3.3. Indoor bio-aerosol distribution – numerical investigations I

In order to further study the bio-aerosol dispersion and explain the above experimental results, the validated CFD model with DPM is applied to 'visualize' the indoor flow and simulate the dispersion and deposition of bio-aerosols. Illustrative planes were obtained by using isosurfaces and the results at height Y = 1.8 m are presented in Fig. 11 (It should be noted that the results at other heights are also examined, which show similar overall trend). As it can be seen in Fig. 11a, the static pressure change inside the poultry building is small due to the relative low air velocity. However, a strong turbulent and disturbed flow is observed at the front part of the house, which results from the side-wall air inlets as shown in Fig. 11b and c. The flow becomes relative steady and uniform at the middle and rear part of the house. Furthermore, the vorticity magnitude, which describes the local spinning motion of a continuum, is illustrated in Fig. 11d. Strong vortex generation and development is noted around the air inlets and the animal occupied zones that close to the inlets. At the downstream of the

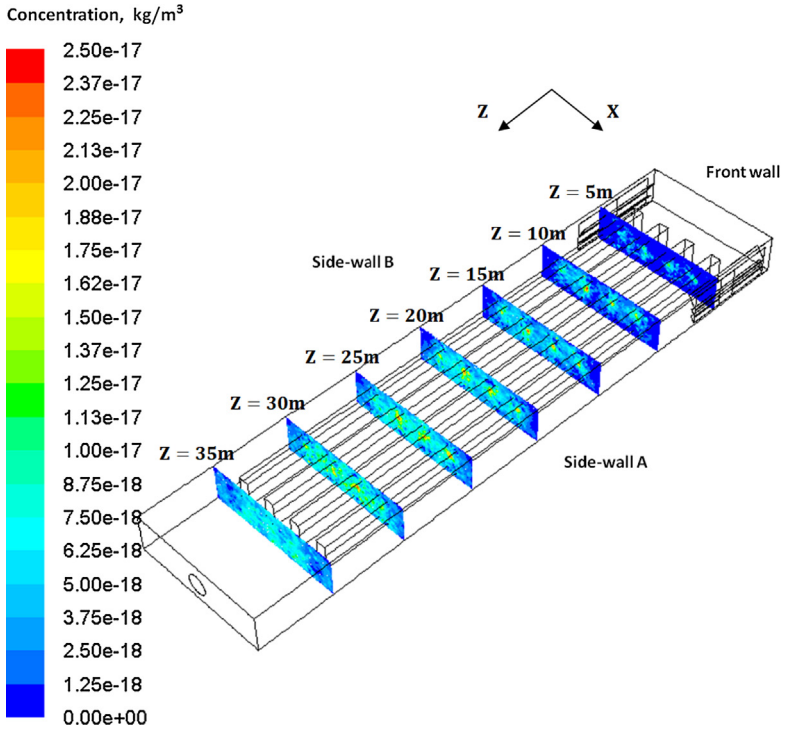

Surface position	Total concentration
Z = 5m	$8.55e^{-15}$
Z = 10m	$2.04e^{-14}$
Z = 15m	$2.67e^{-14}$
Z = 20m	$3.43e^{-14}$
Z = 25m	$4.16e^{-14}$
Z = 30m	$5.45e^{-14}$
Z = 35m	$3.44e^{-14}$

Fig. 12. CFD simulated indoor bio-aerosol concentration (D = 100 μm) at different locations (Z planes), Unit: kg/m^3.

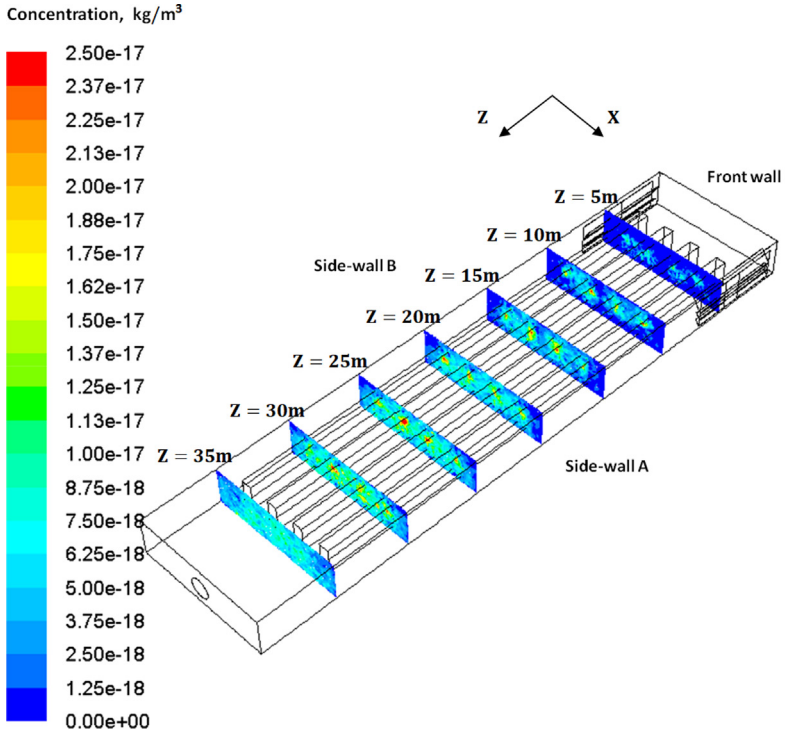

Surface position	Total concentration
Z = 5m	$8.47e^{-15}$
Z = 10m	$2.11e^{-14}$
Z = 15m	$2.86e^{-14}$
Z = 20m	$3.66e^{-14}$
Z = 25m	$4.64e^{-14}$
Z = 30m	$6.15e^{-14}$
Z = 35m	$4.12e^{-14}$

Fig. 13. CFD simulated indoor bio-aerosol concentration (D = 1 μm) at different locations (Z planes), Unit: kg/m^3.

house, the vorticity becomes negligible.

Isosurfaces of indoor bio-aerosol (D = 100 μm) concentrations and distributions at several locations are shown in Fig. 12. When the animal occupied zones are regarded as the sources of bio-aerosols, the simulation results clearly indicate that the concentration of the bio-aerosols gradually increase from the front part of the occupied zone (Z = 5 m, total concentration is 8.55 e^{-15}) to the rear part of the occupied zone (Z = 30 m, total concentration is 5.45 e^{-14}). A noticeable diffusing phenomenon could also be seen in the X direction in Fig. 12 that the bio-aerosols generated from the middle of the occupied zones would diffuse to the aisles next to the side walls (Aisle 1 and Aisle 5). At Z = 5 m limited bio-aerosol concentrations are predicted at Aisle 1 and Aisle 5. However, the strong turbulent flow at the front of the house (see Fig. 11) promote the dispersion of the bio-aerosols and significant amount of bio-aerosol concentrations are already found at Aisle 1 and Aisle 5 for planes of Z = 15 m and Z = 20 m. The overall trend of bio-

Table 6
Number of trapped bio-aerosols for different diameters.

Bio-aerosol diameter	Trapped	Escaped	Percentage of deposition
1 μm	1270	2730	31.7%
5 μm	1258	2742	31.5%
10 μm	1297	2703	32.4%
100 μm	1778	2222	44.5%

Note: the number of trapped bio-aerosols is the mean value of 3 runs.

aerosol dispersion inside the poultry house predicted by the CFD model matches the experimental measurement at Z = 24 m as shown in Figs. 7–9, which indicate the bio-aerosol concentrations at the middle aisles are higher than those at aisles next to the side walls.

The investigations are performed for bio-aerosols with smaller diameters (D = 1 μm, 5 μm, and 10 μm) and the simulation result for D = 1 μm is illustrated in Fig. 13. Comparing with D = 100 μm, the smaller bio-aerosols all demonstrate similar overall dispersion and diffusion patterns. Nevertheless, it is noted that the total concentration for D = 1 μm is higher than that for D = 100 μm at all Z planes examined except Z = 5 m, indicating less deposition on surfaces (walls) at downstream of the house.

An interesting point that should be noted is the bio-aerosol concentration at Z = 35 m is always lower than that at Z = 30 m as shown in Figs. 12 and 13. The plane of Z = 35 m is outside the animal occupied zone which indicate there is no bio-aerosol source and all the bio-aerosols detected come from upstream. A reasonable explanation is that during the dispersion and diffusion parts of the bio-aerosols deposit on the surfaces and the 'trap' boundary condition applied in the CFD model indicates no re-suspension would occur. Without any supplement from sources the total concentration would decrease for planes that outside the occupied zone at the rear part of the house. By tracking all the bio-aerosol sources created in the model, it is possible to know the number of trapped and escaped (emitted) bio-aerosols and a summary table is provided in Table 6. For smaller bio-aerosols with diameters of D = 1 μm, D = 5 μm and D = 10 μm, similar results are predicted as can be seen in Table 6. However, the number of trapped bio-aerosols for D = 100 μm is significantly higher and almost half of the bio-aerosols deposit on the solid walls.

In conclusion, the above CFD simulation results have been shown to compare well to the overall distribution trend of bio-aerosol concentration measured experimentally. Turbulent flow (or disturbed flow) would enhance the dispersion and diffusion of the airborne bio-aerosols. Moreover, bio-aerosols with diameter less than 10 μm are shown to be less likely to deposit on surfaces, which suggests higher risks of indirect contact transmission of pathogen especially for long tunnel-ventilated poultry houses.

3.4. Indoor bio-aerosol distribution – Numerical investigations II

As shown in Figs. 7–9 and Table 5, the experimental measurements indicate the concentration of bio-aerosols at Z = 39.5 m is higher than that at Z = 24 m for each aisle. However, it seems that the CFD model overestimates the particle deposition and the concentration predicted by CFD at Z = 39.5 m is lower than that at Z = 24 m (see Fig. 14). In reality, it is highly possible for small settled bio-aerosols to re-suspend due to the activity of caged birds, local turbulence and disturbed flow, but the re-suspension is not allowed in CFD. Especially, for a tunnel-ventilated poultry house with side-wall air inlets as shown in present study the flow is highly turbulent at the front part of the house (see Fig. 11b), resulting in those small-scale (1 μm) bio-aerosols would not easily settle on surfaces but travel much farther than the CFD predicted.

Moreover, in order to investigate the relative high concentration at the end corners of the poultry house as observed during experimental measurements (see Figs. 7–9 for Aisle 1 and Aisle 5), the simulated velocity vectors at end of the house for Y = 0.8 m and Y = 1.8 m are examined. Meanwhile, a group of bio-aerosols were released around the sampling point 6 (6*) and point 10 (10*) to study the local bio-aerosol

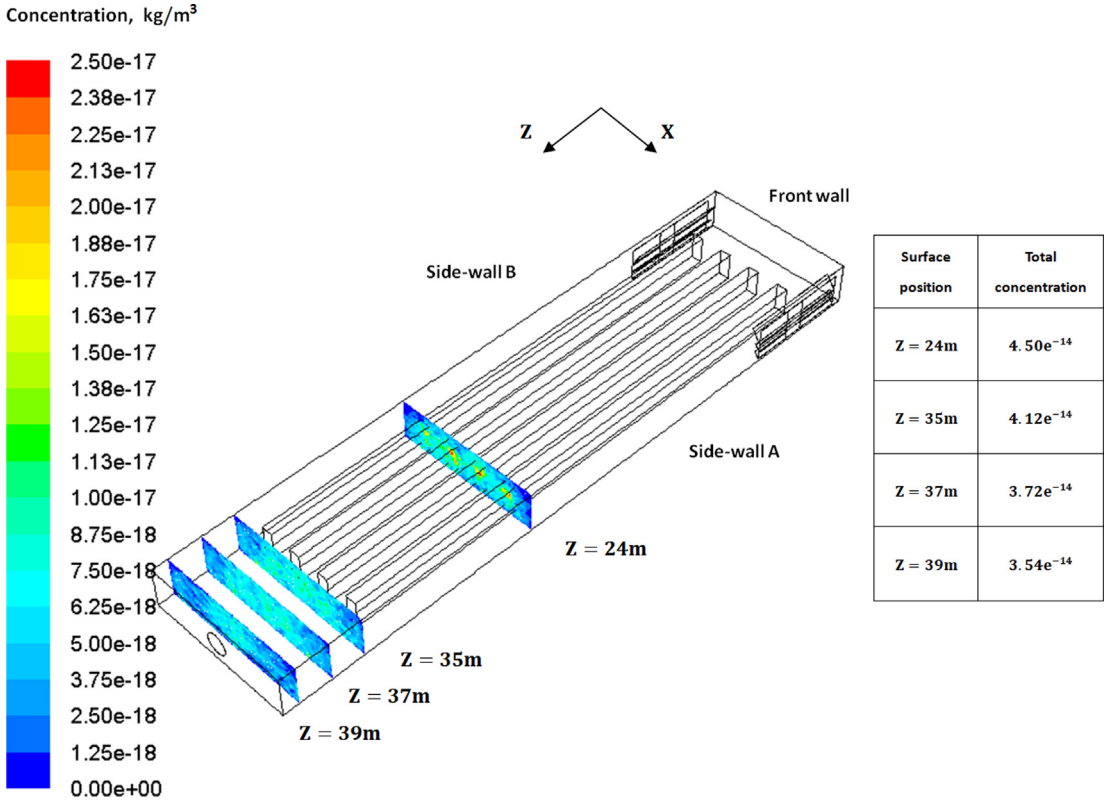

Fig. 14. CFD simulated indoor bio-aerosol concentration (D = 1 μm) at end of the poultry house, Unit: kg/m^3.

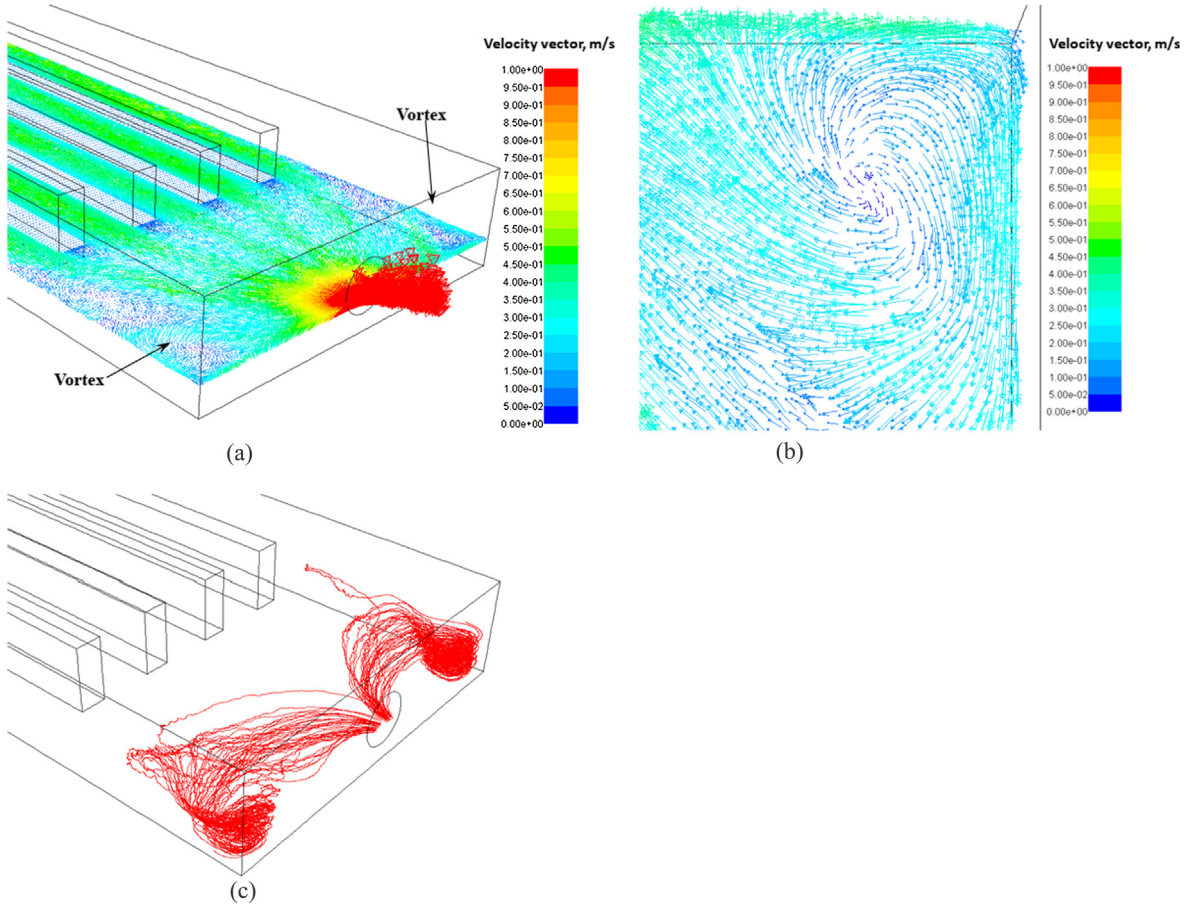

Fig. 15. Simulated results at Y = 0.8 m for (a) velocity vector, m/s (b) enlarged view of velocity vector at the corner, m/s, (c) dispersion pattern of a group of bio-aerosols.

dispersion behaviors. The results are illustrated in Fig. 15. The velocity vector predicted by CFD model at Y = 0.8 m (Fig. 15a) clearly demonstrate a strong disturbed flow region with vortex (eddies) around the end corners of the house. Although the velocity at the center of the vortex is very small, the velocity magnitude around the edge of the vortex is relatively high (see Fig. 15b), which might re-suspend the small-scale settled particles from the solid surfaces in reality. By tracking the bio-aerosols released at the end corners as shown in Fig. 15c, it is found that approximately 25% of the bio-aerosols are 'trapped' by walls and 75% are 'escaped' from the outlet fan. This apparently high deposition percentage indicates that bio-aerosols from upstream would not easily 'escape' to the outside through the ventilation system once they enter the vortex or the disturbed flow region. The dispersion pattern with a vortex-like behavior as shown in Fig. 15c is highly possible responsible for an accumulated high bio-aerosol concentrations as measured in the experiments at the corners. With regard to the simulation results at Y = 1.8 m, no clear vortex is observed at the corners but the flow is also highly disturbed, resulting in approximately 15% of the released bio-aerosols deposit on walls.

In conclusion, the re-suspension of small-scale bio-aerosols is highly possible to occur under such a complex and turbulent indoor flow in tunnel-ventilated poultry houses, although deposition is overestimated in CFD due to the 'trapped' boundary condition. Local vortex and disturbed flow would further contribute to an increased local concentration of bio-aerosols in reality and therefore special attentions should be paid to these locations during cleaning or disinfection. Meanwhile, efforts could be made to avoid the occurrence of disturbed flow region during the poultry house design stage.

4. Conclusions

In order to fill a gap of the understanding of bio-aerosol distribution, dispersion and deposition in a tunnel-ventilated poultry house, a 3-dimensinal CFD model is successfully built and validated in present study. The CFD model with DPM (Discrete phase model) is demonstrated to be able to visualize the trend of dispersion pattern of bio-aerosols, indicating areas of higher or lower concentrations, rather than a total or representative biological count in the house. The overall trend from the model prediction matches well with the experimental measurements although no special effort is made in CFD model to exactly match the bio-aerosol generation rate and release locations in the poultry house. According to the results from this paper, possible optimization could be conducted both at the poultry house design and operation stage to reduce the bio-aerosol concentration.

Based on present study some conclusions can be drawn as follow:

- For tunnel-ventilated poultry houses, higher concentrations of bio-aerosols are expected at the rear part of the house.
- Turbulent flow or disturbed flow resulting from the configuration of the ventilation system enhances the bio-aerosol dispersion and re-suspension. A uniform indoor flow pattern might be more suitable for poultry houses from the standing point of reducing airborne bio-aerosols.
- Local disturbed flow region or vortex region inside the poultry houses should be treated carefully during cleaning and disinfection since bio-aerosols could re-suspend and accumulate at these locations.
- Deposition is a localized process which depends strongly on both flow pattern and aerosol physical properties (e.g. diameter). Based

on present study, bio-aerosols with diameter less than 10 μm show similar dispersion and deposition behavior while larger bio-aerosols (D = 100 μm) is more likely to deposit on surfaces.

- The CFD model overestimates the bio-aerosol deposition due to the 'trapped' boundary condition while re-suspension could occur in reality in poultry houses due to the complex flow conditions and the activity of birds.

Declaration of Competing Interest

The authors declared that there is no conflict of interest.

Acknowledgement

This work was supported by the Sichuan Science and Technology Program (No. 2019YFN0009); the National Key Research and Development Project (No. 2016YFD0500510); the province key technologies R&D program of livestock and poultry breeding programs of Sichuan province (No. 2016NYZ0043).

References

Al Homidan, A., Robertson, J.F., Petchey, A.M., 1997. Effect of temperature, litter and light intensity on ammonia and dust production and broiler performance. Br. Poult. Sci. British Poultry Sci. 38, S5–S17.

Banhazi, T.M., Seedorf, J., Laffrique, M., Rutley, D.L., 2008. Identification of the risk factors for high airborne particle concentrations in broiler buildings using statistical modelling. Biosyst. Eng. 101, 100–110.

Banhazi, T., Seedorf, J., Rutley, D.L., Pitchford, W.S., 2008. Identification of risk factors for sub-optimal housing conditions in Australian piggeries – part III: environmental parameter. J. Agric. Safety Health 14, 41–52.

Banhazi, T., Seedorf, J., Rutley, D.L., Pitchford, W.S., 2008. Identification of risk factors for sub-optimal housing conditions in Australian piggeries – part II: airborne pollutants. J. Agric. Safety Health 14, 41–52.

Blanes-Vidal, V., Guijarro, E., Balasch, S., Torres, A.G., 2008. Application of computational fluid dynamics to the prediction of airflow in a mechanically ventilated commercial poultry building. Biosyst. Eng. 100 (1), 105–116.

Brodka, K., Kozajda, A., Buczyńska, A., Szadkowska-Stańczyk, I., 2012. The variability of bacterial aerosol in poultry houses depending on selected factors. Int. J. Occup. Med. Environ. Health 25 (3), 281–293.

Cambra-Lopez, M., Aarnink, A.J.A., Zhao, Y., Calvet, S., Torres, A.G., 2010. Airborne particulate matter from livestock production systems: a review of an air pollution problem. Environ. Pollut. 158, 1–17.

Cheng, Q., Wu, W., Li, H., Zhang, G., Li, B., 2018. CFD study of the influence of laying hen geometry, distribution and weight on airflow resistance. Comput. Electron. Agric. 144, 181–189.

Du, L., Yang, C., Dominy, R., Yang, L., Hu, C., Du, H., Li, Q., Yu, C., Xie, L., Jiang, X., 2019. Computational Fluid Dynamics aided investigation and optimization of a tunnel-ventilated poultry house in China. Comput. Electron. Agric. 159, 1–15.

Kirychuk, S., Senthilselvan, A., Dosman, J.A., Juorio, V., Feddes, J.J., Wilson, P., Classen, H., Reynolds, S.J., Guenter, W., Hurst, T.S., 2003. Respiratory symptoms and lung function in poultry confinement workers in Western Canada. Canadian Respir. J. 10 (7), 375–380.

Lai, A., Chen, F., 2006. Modeling particle deposition and distribution in a chamber with a two-equation Reynolds-averaged Navier-Stokes model. Aerosol Sci. 37, 1770–1780.

Mostafa, E., Buescher, W., 2011. Indoor air quality improvement from particle matters for laying hen poultry house. Biosyst. Eng. 109, 22–36.

Nimmermark, S., Lund, V., Gustafsson, G., Eduard, W., 2009. Ammonia, dust and bacteria in welfare-oriented systems for laying hens. Ann. Agric. Environ. Med. 16 (1), 103–113.

Oppliger, A., Charriere, N., Droz, P.-O., Rinsoz, T., 2008. Exposure to bioaerosols in poultry houses at different stages of fattening; use of real-time PCR for airborne bacterial quantification. Annal. Occupat. Hygiene 52 (5), 405–412.

Qi, R., Manbeck, H.B., Maghirang, R.G., 1992. Dust generation rate in a poultry layer house. Trans. ASAE 35, 1639–1645.

Roache, P., 1994. Perspective: a method for uniform reporting of grid refinement studies. J. Fluids Eng.-Trans. ASME 116 (3), 405–413.

Rong, L., Nielsen, P.V., Bjerg, B., Zhang, G., 2016. Summary of best guidelines and validation of CFD modeling in livestock buildings to ensure prediction quality. Comput. Electron. Agric. 121, 180–190.

Saleh, M., Seedorf, J., Hartung, J., 2003. Total count of bacteria in the air of three different laying hen housing systems. Dtsch. Tierarztl. Wochenschr. 110 (9), 394–397.

Vučemilo, M., Matković, K., Vinković, B., Jakšić, S., Granić, K., Mas, N., 2007. The effect of animal age on air pollutant concentration in a broiler house. Czech J. Animal Sci. 52 (6), 170–174.

Zhao, B., Zhang, Y., Li, X., Yang, X., Huang, D., 2004. Comparison of indoor aerosol particle concentration and deposition in different ventilated rooms by numreical mothod. Build. Environ. 39, 1–8.